The Origin of Phototrophy Reveals the Importance of Priority Effects for Evolutionary Innovation

Anthony Burnetti[1,2],William C. Ratcliff[1]

[1]*Georgia Institute of Technology, School of Biological Sciences, Atlanta, GA, USA.*

[2]*Corresponding Author: anthony.burnetti@biosci.gatech.edu*

Running title: Imprints of Priority Effects on Evol. Innovation

Author contributions: Anthony Burnetti conceived and performed the majority of research and analysis presented in this paper, with William Ratcliff contributing significant revisions.

Acknowledgements: This work was supported by NSF grants IOS-1656549 and DEB-1845363, and a Packard Foundation Fellowship to W.C.R

Data accessibility statement: There is no novel data to be archived represented in this publication.

Preprints (www.preprints.org) | NOT PEER-REVIEWED | Posted: 31 August 2022 doi:10.20944/preprints202011.0700.v4

The history of life on Earth has been shaped by a series of major evolutionary innovations. While some of these innovations occur repeatedly, some of the most important innovations are evolutionary singularities, arising only once. This fact has often been interpreted to mean that singularities are particularly difficult, low-probability evolutionary events, implying the long-term course of life on Earth is highly contingent. Alternatively, singularities could arise from evolutionary priority effects, where first-movers suppress subsequent independent origins. Here, we disentangle these hypotheses by examining the origins of phototrophy. The ability to use light for energy evolved independently twice, preserving information about their origins that is lost when examining singularities. We show that the two forms of phototrophy occupy opposite ends of key trade-offs: most importantly efficiency of light capture vs. return on investment. Our results suggest that the 'dual singularity' of phototrophy exists due to evolutionary interactions between nascent phototrophs, within a phototrophic niche space too large for a single first mover to fill all niches and fully suppress all future innovation. While often ignored over geological time scales, ecological interactions and evolutionary priority effects may play a fundamental role in the tempo and mode of major evolutionary innovations.

1 Introduction

Life has been profoundly shaped by a series of evolutionary innovations. From the origin of life via prebiotic chemistry in the Hadean through to the more recent evolution of multicellular organisms, these innovations have extended the upper reaches of organismal complexity and fundamentally changed the state of the biosphere. Some critical innovations have recurred many times across the tree of life, while others have occurred just once in all of history. Given their impact on ecological and evolutionary dynamics, understanding the origin and spread of key biological innovations is fundamental to understanding history of life on Earth.

Some major evolutionary innovations have occurred many times. Multicellularity, for instance, is ubiquitous on today's Earth and has evolved at least 25 times from unicellular ancestors[1] with complex multicellularity has evolved at least five to six times among the metazoans, embryophytes, red algae, brown algae, and fungi[2–4]. Putative multicellular fossils are observed all the way back to 2.1-2.4 billion years ago[5,6], indicating that this innovation has a long history. Other evolutionary transitions in individuality have also evolved repeatedly in diverse lineages, including endosymbiosis and superorganismality[7], as have innovations such as C4 photosynthesis[8] and tetrapod powered flight[9]. Given their repeated evolution, none of these innovations appear to be evolutionarily 'difficult'.

Several of the most important innovations and transitions in the history of life, however, are those which have apparently occurred only once (Figure 1). The origin of life from abiotic chemistry is arguably the most important evolutionary innovation in history, along with the nearly immediate origin and crystallization of the genetic code and a system of stable heredity[10]. The origin of eukaryotes via a symbiosis between an archaea and proteobacterium[11,12] was then perhaps one of the most impactful single innovation since life's origin. Eukaryogenesis is often considered to have been highly contingent on chance events, more than any other transition. Lane et al. call it a restrictive, singular bottleneck[13] by which an unlikely event (endosymbiosis of mitochondria) is a prerequisite for complex life of any kind[14]. The existence of such unique impactful innovations has

Preprints (www.preprints.org) | NOT PEER-REVIEWED | Posted: 31 August 2022 doi:10.20944/preprints202011.0700.v4

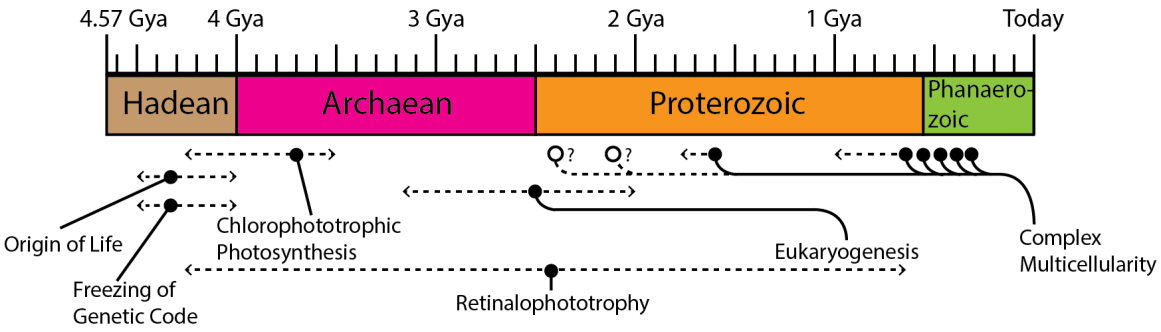

Figure 1: **The history and approximate timing of major innovations and evolutionary transitions in Earth's biosphere.** The origin of life, the freezing of the genetic code, and eukaryogenesis are evolutionary singularities as they were major innovations which occurred just once. Complex multicellularity has evolved repeatedly across at least the last 1.6 billion years[2,3,5]. Phototrophic metabolism has evolved twice, via chlorophototrophy and retinalophototrophy. Chlorophototrophy dates to at least 3.5 billion years ago with the oldest unequivocal fossil photosynthetic microbial mats[16,17], though some argue for older dates[18]. The origin of retinalophototrophy is uncertain due to its lack of preservation in the fossil record, and could date from anywhere between the Hadean to shortly before the rise of animals, but is more likely to be ancient[1920]. The dual origins of phototrophy provides unique insight into the nature and process of evolutionary innovation.

led some to conclude that the history of life on Earth is sensitive to the presence and timing of these rare events, and that most possible biospheres would therefore not possess the complexity and scale that ours does[15].

These evolutionary singularities are notoriously difficult to study[21]. They could of course represent extremely rare chance events or restrictive bottlenecks that we only see due to anthropic selection effects[15]. But they could also represent 'frozen accidents' by which a single lineage experienced a winner-take-all effect, deterministic necessities which could only occur one way, or could be the result of evolutionary attrition in which a large number of original innovators were winnowed down stochastically over time[21]. Unfortunately, there is little information left in the modern day, hundreds of millions or billions of years after the singular event occurred, that would allow us to distinguish between these mechanisms. In this paper, we circumvent these limitations by examining the evolution of phototrophy (the ability to use light as a metabolic energy source), which has independently evolved twice and thus retains information about its origin that has been lost in evolutionary singularities.

The evolution of phototrophy is one of the most significant events in the history of life on Earth. It is one of the oldest evolutionary innovations discussed here, occurring at least 3.5 billion years ago[16,17] with some arguing for earlier dates[18]. The capture of light energy into metabolism allowed an enormous increase in the scale of Earth's biosphere. Without the use of radiant light energy to power metabolism in phototrophs and build biomass in photosynthesizers, the only reasonable mechanism for primary production by the early biosphere was chemolithoautotrophy utilizing geologically and atmospherically produced redox couples[22,23]. This puts a low ceiling on the potential primary production of biomass in a nonphotosynthetic biosphere (supplemental

Preprints (www.preprints.org) | NOT PEER-REVIEWED | Posted: 31 August 2022 doi:10.20944/preprints202011.0700.v4

figure 1). Photosynthesis is thus the key factor allowing the existence of the large, high-biomass, geochemically significant modern biosphere, transforming the composition of both the atmosphere[24] and the geosphere[25] over geological time.

Unlike other biosphere-transforming innovations, the ability to use light for metabolic energy appears to have evolved independently twice, via mechanisms known as retinalophototrophy and chlorophototrophy[26]. As the only such 'dual singularity', it preserves information on the evolutionary factors underpinning the origin of rare, impactful innovations that have been lost in true singularities. Here we present a mathematical analysis of the trade-offs in energy transduction performed by modern phototrophic metabolisms, and a mathematical model of the trade-offs inherent in their evolution from less sophisticated and diverse ancestors. By examining their relationships and apparent evolutionary histories, we find that chlorophototrophy and retinalophototrophy have partitioned phototrophic niche space between themselves. They occupy opposite ends of essential trade-offs between efficiency per unit resource versus efficiency per unit infrastructure, use of rare limiting nutrients versus metabolic versatility, and complexity versus simplicity. This deep complementarity suggests that phototrophy has evolved only twice not because this innovation is intrinsically difficult but because phototrophic niche space is too large for an initial first mover to fully suppress future innovation, but too small to support many separate innovations. Together, this work highlights the critical role of evolutionary priority effects in the evolution of biological innovations, and suggests that the origins of evolutionary singularities may be less constrained or contingent than is widely believed.

2 Background - Chlorophototrophy and Retinalophototrophy

Here we provide a brief review of Earth's two major phototrophic metabolic pathways, which will provide necessary context for our results below. For a more detailed review of chlorophototrophy, retinalophototrophy, their likely evolutionary histories, and the trade-offs inherent to their structures, see supplement s1.

The first phototrophic metabolism to be studied is known as chlorophototrophy. Named for the chlorophyll and bacteriochlorophyll pigments that absorb light, chlorophototrophs drive both energy metabolism and redox chemistry via light. Found in cyanobacteria, eukaryotes that took up plastids, and at least seven other phototrophic clades of bacteria[27,28], it is responsible for the vast majority of primary production of biomass on Earth as well as much of the energy metabolism of organisms which possess it. Approximately 9,000 teramoles of carbon are fixed by chlorophototrophs annually[29], primarily via oxygenic photosynthesis (supplemental figure 1).

The functional unit of the chlorophototrophic machinery is the photochemical reaction center, or RC. These membrane-bound protein complexes are large, massing hundreds of kilodaltons and containing a minimum of eight pigment/cofactor molecules[30,31]) and are all descended from an ancestral homodimer[32]. In addition to their defining pigments all reaction centers contain iron in the form of iron-sulfur clusters, single coordinated iron atoms, or hemes bound to integral cytochromes [28,33–39]. All chlorophototrophic reaction centers push electrons to more reducing potentials via chlorophyll and bacteriochlorophyll photochemistry. They may pass these electrons to ferredoxin electron carriers which can be used to fix biomass to carbon fixation pathways, or energize an electron transport chain to produce biologically available energy in the form of proton gradients and

Preprints (www.preprints.org) | NOT PEER-REVIEWED | Posted: 31 August 2022 doi:10.20944/preprints202011.0700.v4

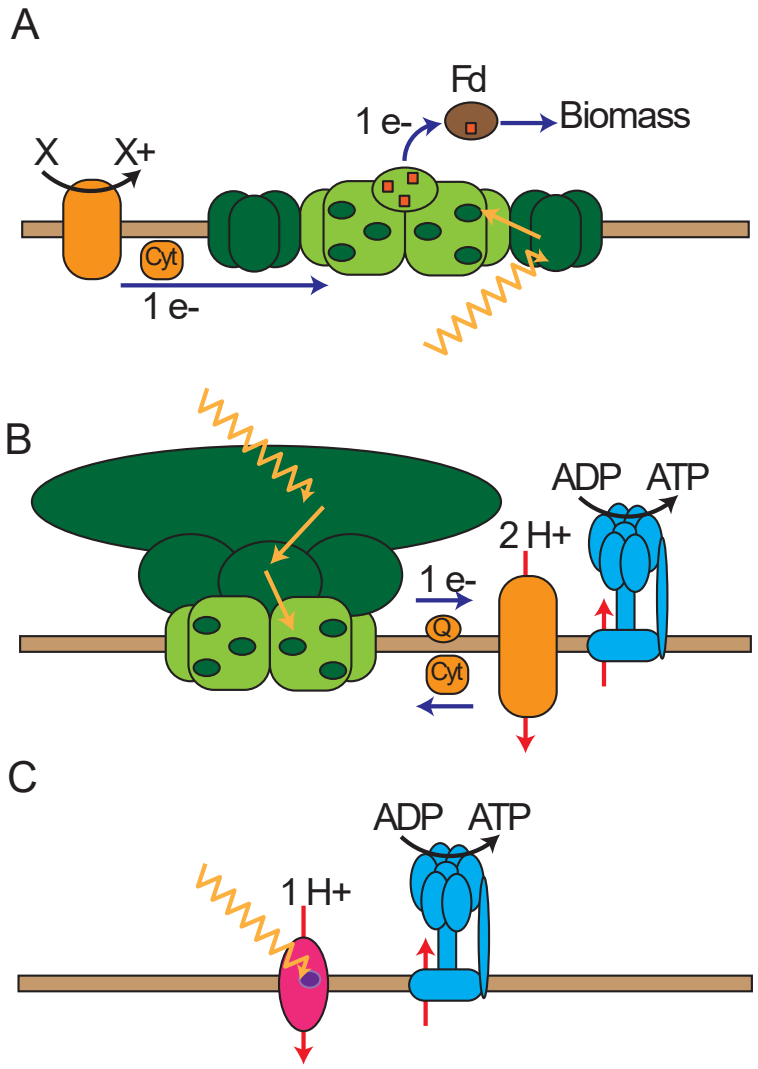

Figure 2: **Simplified illustration of the main types of phototrophic metabolism. A)** Chlorophototrophy, type I reaction center. A photon is absorbed by one of a diverse array of antenna complexes (dark green) and passed as an exciton via Förster resonance to chlorophyll or bacteriochlorophyll molecules (small dark green spots) within the dimeric photosynthetic reaction center (light green). A type I reaction center is illustrated acquiring an electron via a cytochrome derived from an environmental reducing agent, boosting it via light energy to a low redox potential, and passing it via iron-sulfur clusters (red) to ferredoxin (brown) which can be used to build biomass via carbon and nitrogen fixation. **B)** Chlorophototrophy, type II reaction center illustrated passing electrons to a quinone electron acceptor, allowing for simple cyclic electron transfer via cytochrome bc1 (complex III) (orange) and the pumping of two protons per absorbed photon. **C)** Retinalophototrophy. A single molecule of retinal (purple) is bound to a microbial rhodopsin membrane protein (pink). Absorption of a photon causes one proton to be pumped the exterior of the cell, upon which it can participate in chemiosmotic ATP production via the membrane ATP synthase (blue).

Preprints (www.preprints.org) | NOT PEER-REVIEWED | Posted: 31 August 2022 doi:10.20944/preprints202011.0700.v4

ATP via chemiosmosis (Figure 2 A,B). Absorption of a single photon typically pumps two protons across the membrane, although in some cases up to four can be pumped[40–42].

All reaction centers couple a conserved central dimeric core to additional pigments in intrinsic 'antenna' complexes of a hundred kilodaltons or more[43,44] which increase the absorption cross section per functional unit by funneling light into the reaction center via Förster resonance transfer. A diverse array of additional accessory antennas[45,46] are further coupled to these central complexes. The quantity of additional antenna pigment per reaction center varies widely between different organisms, with adaptation to different light levels accounting for much of the difference.

The retinalophototrophic system, only discovered in the 1970s via investigation of the phototrophic mechanism of haloarchaea[47], is far simpler than chlorophototrophy. It consists of a single 26-28 kilodalton transmembrane protein, known as a microbial or 'type-1' rhodopsin (Figure 2 C). It is covalently bound to a single pigment molecule known as retinal, derived from the oxidative splitting of a carotenoid via a dioxygenase[48]. In a few cases, such as the xanthorhodopsins, a single additional carotenoid molecule is bound to the exterior of the protein and functions as a miniature integral 'antenna'[49] but rhodopsins are not known to be associated with accessory antennas. Rather than participating in redox chemistry they directly pump protons across the cell membrane driven by light-induced isomerization of the retinal pigment molecule[50]. Rhodopsins cannot be used to fix inorganic carbon into biomass because they fail to push membrane to a high enough voltage for reverse electron flow[51], but still generate large amounts of biological energy. The quantity of light absorbed by retinalophototrophs in the ocean is thought to be at least as large as that absorbed by chlorophototrophs[52].

In contrast to a pattern of inheritance of chlorophototrophy primarily explained by vertical transmission with occasional, exceptional moments of horizontal transfer[53], retinalophototrophy is often transferred horizontally. It is found in all three domains of life and in a significant fraction of heterotrophic bacteria in the ocean[47,54–61]. This is likely due to its relatively low cost, as it is composed of small proteins, does not require metal ions, and can function even without an electron transport chain. Further, the genes underlying retinalotrophy are small and easily horizontally transferred, requiring a maximum of five separate genes (frequently encoded in a conserved cluster) for a functional pump/pigment synthesis system, compared to 30 or more for chlorophototrophy[62–64].

While the diversity and fine molecular details of the modern diversity of each of these systems is immense, their most outstanding differences can be summed up simply - their composition, their output, and their ability to intercept light. As illustrated in Figure 3, chlorophototrophy uses a large protein complex containing iron while retinalophototrophy uses a small protein complex without a metal cofactor. Phototrophic reaction centers are capable of outputting either energy or biomass, while rhodopsins are only able to produce energy and produce less energy per photon. Lastly, with their large antenna pigments chlorophototrophs can intercept a larger flux of photons per functional unit that retinalophototrophs can.

How have these two distinct phototrophic systems managed to coexist across the deep history of Earth, what is their ecological relationship, and what does this relationship tell us about their origins and the process of innovation that drove phototrophy into existence? We seek to gain insight into these questions by quantitatively comparing the trade-offs which characterize extant phototrophs.

Preprints (www.preprints.org) | NOT PEER-REVIEWED | Posted: 31 August 2022 doi:10.20944/preprints202011.0700.v4

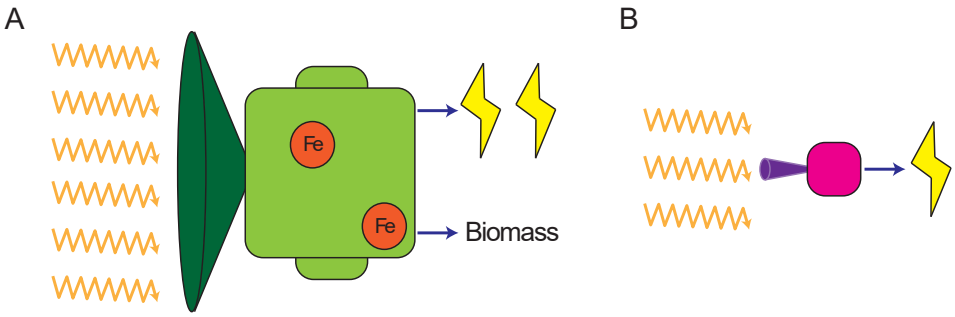

Figure 3: **Schematic illustrating key functional differences between retinalophototrophy and chlorophototrophy. A)** Chlorophototrophic functional units have high absorption cross sections due to light-gathering antenna pigments (dark green), high protein mass per functional unit (light green), use iron ions in their internal structure (orange) in addition to protein and organic pigments, and either conserve large amounts of energy per photon or are capable of contributing to biomass production. **B)** Functional units in retinalophototrophy have small absorption cross sections (purple), little protein mass (pink), and conserve low energy per photon.

3 Results

Modern chlorophototrophs and retinalophototrophs

All metabolic machinery carries with it an investment cost in protein mass - the infrastructure must be built before it can transduce energy or nutrients, and has a finite lifetime before being either recycled or diluted away by growth and division. As such every metabolic pathway also has a rate of return on investment, defining a major aspect of its physiological function and ecological role. We begin by examining the physiology of extant phototrophs, as they have been extensively characterized.

We first calculated an effective specific energy flux per unit protein investment of different phototrophic systems based on a literature review of vital parameters for anoxygenic chlorophototrophic RCs, oxygenic RCs, and two different microbial rhodopsins (proteorhodopsin and bacteriorhodopsin)[30,35,42,47,51,65–78]. Vital parameters included total protein mass per functional unit M_{total} in kDa, the maximum rate R_{max} in cycles per second, protons pumped per cycle N_p, and the light level at which absorption is at half-maximum, K_m, in units of micromoles of photons per square meter per second. Using equation 1 we calculated the maximum flux per unit protein at saturating light levels V_{max} (protons per kilodalton per second) (See Table 1, and supplemental equation S1).

Equation 1:

$$V_{\max} = \frac{N_{\mathrm{p}} \cdot R_{\max}}{M_{\mathrm{total}}}$$

Despite their higher energy yield per photon absorbed and faster photocycle, chlorophototrophic machinery is so much more massive than microbial rhodopsins that their specific energy flux per unit mass is significantly lower. We calculate that proteorhodopsin and bacteriorhodopsin are 2.78-fold and 11.53-fold more efficient per unit investment than oxygenic RCs, respectively, with anoxygenic RCs roughly equivalent to oxygenic RCs (Table 1 Figure 4 A, and supplement S2).

Preprints (www.preprints.org) | NOT PEER-REVIEWED | Posted: 31 August 2022 doi:10.20944/preprints202011.0700.v4

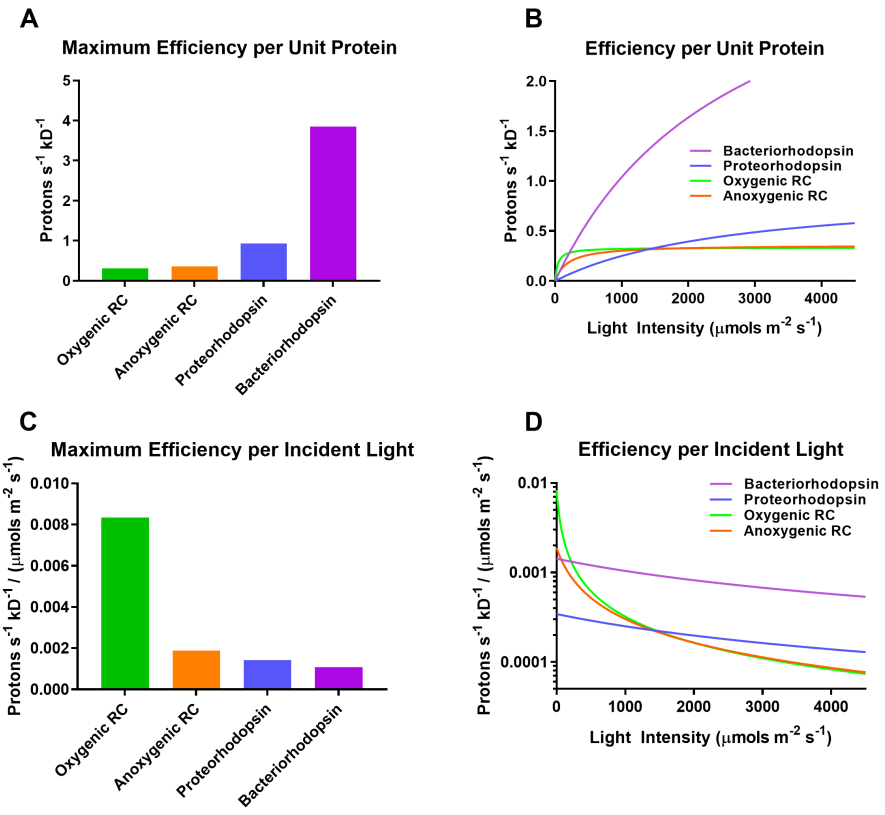

Figure 4: **Physiological comparison between modern chlorophototrophs and retinalophototrophs.** **A)** Calculated maximum pumped proton flux available per kDa of protein mass of anoxygenic purple bacterial reaction centers, oxygenic reaction centers, proteorhodopsin, and bacteriorhodopsin at saturating levels of light. Microbial rhodopsins saturate at much higher specific metabolic energy fluxes than chlorophototrophic reaction centers. **B)** Calculated proton flux available per kilodalton of mass of different modern phototrophic systems at different light intensities. Chlorophototrophic reaction centers produce more energy flux at low light levels compared to microbial rhodopsins, but saturate quickly, while microbial rhodopsins function best at high light levels with higher specific metabolic energy fluxes. **C)** Calculated maximum pumped proton flux available per kDa per unit incident light in microeinsteins per square meter. Chlorophototrophic reaction centers are capable of extracting much more energy flux per unit incident light. **D)** Calculated energy flux per kilodalton of machinery per microeinstein of incident light. Chlorophototrophic reaction centers are significantly more efficient per unit incident light when light is scarce, but rapidly saturate due to having large absorption cross sections per reaction center, thereby gathering more light than can be converted to energy. Microbial rhodopsins are significantly less efficient per photon, but use light more efficiently than chlorophototrophy when light levels are high. See supplement S2 for our calculations and model parameters derived from a review of the literature.

Preprints (www.preprints.org) | NOT PEER-REVIEWED | Posted: 31 August 2022 doi:10.20944/preprints202011.0700.v4

Table 1: Energy Flux Per Unit Mass of Modern Chlorophototrophs and Retinalophototrophs

	Anoxygenic RC	Oxygenic RC	Proteorhodopsin	Bacteriorhodopsin
Total protein mass / unit	~835 kDa	~2098 kDa	27 kDa	26 kDa
Electrons s^{-1}	~150	~350	0	0
Protons s^{-1}	~300	~700	~25	~100
Protons s^{-1} kDa^{-1}	0.36	0.33	0.92	3.85
Normalized protons s^{-1} kDa^{-1}	1.08	1	2.78	11.53

Proton flux per unit protein mass available to different phototrophic machineries at full light saturation. See supplement S2 for calculations.

We extended this analysis from the maximal energy flux per unit mass to the flux per unit mass at differing light levels based on the absorption cross section and maximum turnover rate of different phototrophic machineries (see supplement S2 and supplemental equation S2). We treated light absorption and conversion as a Michaelis-Menten process resulting in equation 2, describing the energy flux per unit protein F_p at a given light intensity L.

Equation 2:

$$F_p = \frac{V_{\max} \cdot L}{K_m + L}$$

We find that the greater return per unit investment for retinalophototrophs only manifests at high light (Figure 4B). The small protein mass and presence of only a single retinal pigment in a microbial rhodopsin ensures a small cross section which requires intense ambient light for the machinery to be used effectively. Conversely, the large absorption cross section available to the much larger chlorophototrophic system is nearly saturated above low light levels of less than approximately 500 micromoles of photons per square meter per second, but at these lower light levels maintains a higher energy flux per unit infrastructure. This implies a greater efficiency per unit ambient light in low light by chlorophototrophs.

By dividing the function of the return per unit investment of each phototrophic system by the level of ambient light, we produced equation 3 describing the efficiency per unit ambient light, F_L, in units of protons pumped per kilodalton per second, per micromole of photons per square meter per second and equation 4 describing the maximum energy flux per kilodalton per unit ambient light Y_{max} (Figure 4C, D and equations S3-S4).

Equation 3:

$$F_L = \frac{V_{\max}}{K_m + L}$$

Equation 4:

$$Y_{\max} = \frac{V_{\max}}{K_m}$$

Preprints (www.preprints.org) | NOT PEER-REVIEWED | Posted: 31 August 2022 doi:10.20944/preprints202011.0700.v4

While modern chlorophototrophic reaction centers are more efficient per unit ambient light in the limit of low light, this is again reversed at higher light levels. Thus, modern chlorophototrophs have both a higher energy flux per unit infrastructure at low light and a higher energy yield per unit ambient light at low light while retinalophototrophs excel at both in high light. Modern chlorophototrophs are however capable of much higher maximum efficiencies per unit light than retinalophototrophs, while modern retinalophototrophs are capable of much higher maximum fluxes per unit protein infrastructure.

Modeling of Trade-offs in the Evolution of Phototrophic Systems

The above analysis broadly indicates Earth's two photosystems are largely dinstingushed by the trade-off between efficiency per unit infrastructure and efficiency per unit incident light. So far, we have utilized data from extant chlorophototrophs and retinalophototrophs. Over the course of their evolution, retinalophototrophs and chlorophototrophs have sampled an enormous variety of configurations in order to adapt to many distinct ecological sub-niches. What is seen in the world today represents phototrophic systems that are highly adapted to their particular environments, rather than everything that these systems are capable of.

In order to examine the theoretical capabilities of retinalophototrophs and chlorophototrophs, and the implications of the trade-offs stemming from either phototrophic system on organismal physiology, evolutionary history, and ecological interactions, we constructed an analytical model of an arbitrary phototrophic system (Figure 5). This model consists of the central catalytic core of the rhodopsin or reaction center with a constant yield, maximum velocity, and absorption cross section. It is parameterized in terms of yield per cycle Y (protons / cycle), maximum rate V_{max} (cycles per second), mass of catalytic core k (kDa), absorption cross section per catalytic core b (Å^2), mass of antenna complexes x (kDa), absorption cross section per unit mass of antenna a (Å^2 kDa^{-1}) photodegradation constant D (photon^{-1}), and recycling rate R (s^{-1}).

The properties of a chlorophototrophic catalytic core were imputed by examining an anoxygenic bacterial type II reaction center[30], and those of microbial rhodopsins from bacteriorhodopsin[66,81]. The catalytic core is paired with antenna complexes of variable size, whose absorption cross section per unit mass is imputed by examination of the LH2 antenna of a purple nonsulfur bacterium[82]. Both chlorophototrophic reaction centers and rhodopsins were allowed to be paired with antenna complexes so as to not limit the model to configurations seen today, where only chlorophototrophs have antenna complexes larger than single carotenoid molecules, which could conceivably be due to historical contingency.

Photodegradation properties are taken from Faizi et al., 2018[83]. All parameters were constrained by previous literature and this photodegradation model except for the rate of recycling and dilution of phototrophic machinery by cell growth and division (R) which is highly dynamic depending on cellular doubling time and metabolic state. We took this value to be 0.1 hr^{-1} in this analysis, corresponding to a protein half life or cellular doubling time of 6.93 hours, as this growth rate is comparable to those observed for rapidly growing chlorophototrophic algae media[84] and close to the upper growth rates modeled in Faizi et al[83]. Varying this recycling and dilution timescale did not qualitatively impact our results - see supplement S2 and supplemental figure 4 for sensitivity analysis. See Table 2 for all variables used in this analysis and supplement S2 for calculations of all numerical variables used from a literature review.

Preprints (www.preprints.org) | NOT PEER-REVIEWED | Posted: 31 August 2022 doi:10.20944/preprints202011.0700.v4

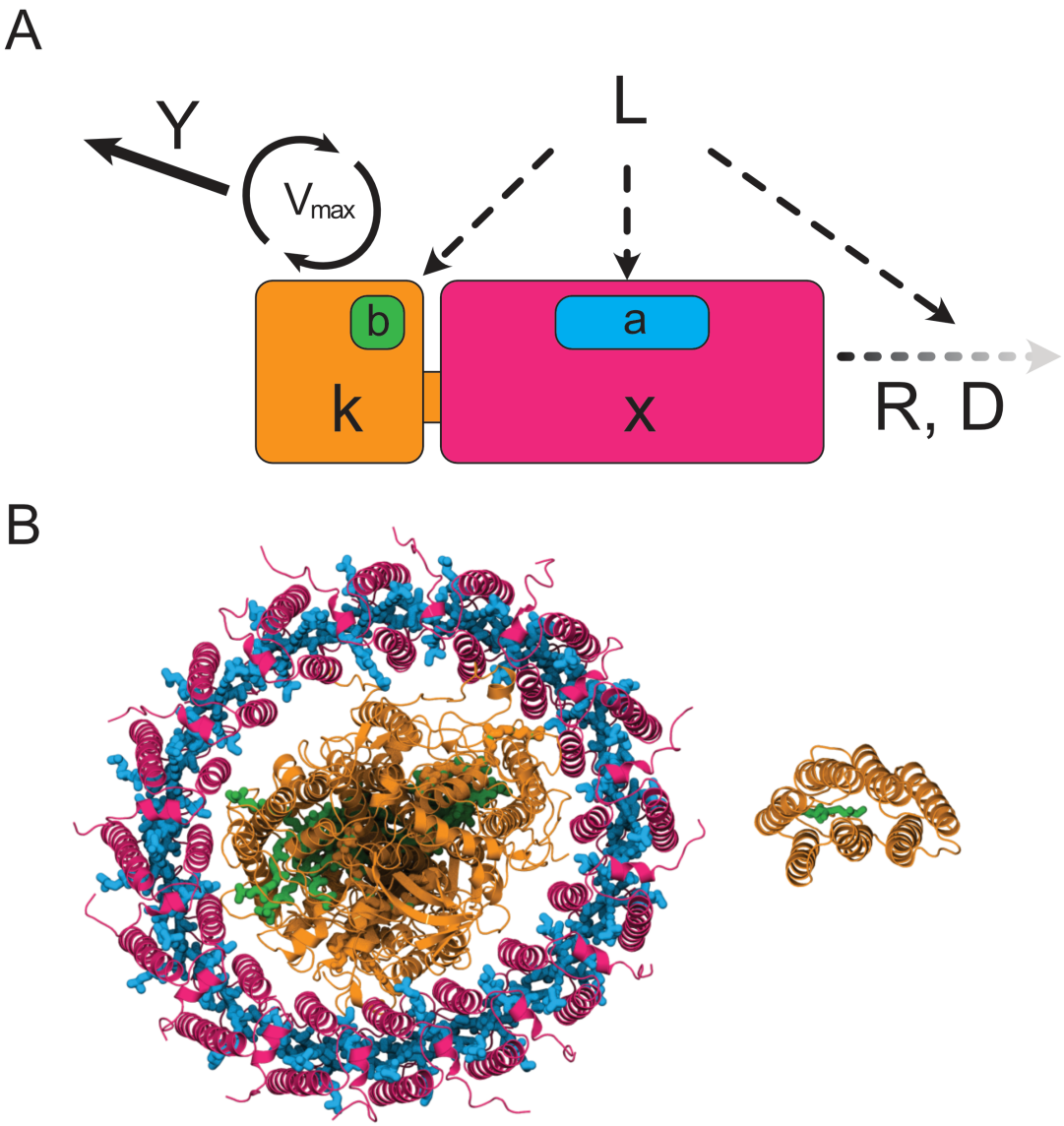

Figure 5: **Modeling trade-offs in the evolution of chlorophototrophy and retinalophototrophy. A)** Model schematic. A central invariant catalytic core for each phototrophic system is pictured in orange, with a mass k. Its maximum reaction speed is V_{max}, with a yield of protons pumped across a membrane per catalytic cycle of Y. It has an intrinsic light absorption cross section of b. This is paired to an antenna of mass x, pictured in magenta. Its absorption cross section per unit mass is represented as variable a. The incident light intensity falling upon the system is represented by the variable L. The protein recycling rate is represented by R, and the photodegradation rate constant is represented by D. **B)** Visualizations of phototrophic machinery using the same color-coding as previously pictured idealized phototrophic machinery. Left, the type II reaction center and LH1 antenna complex from *Thermochromatium tepidum*[44], right, bacteriorhodopsin[79]. Created with Protein Imager[80].

Preprints (www.preprints.org) | NOT PEER-REVIEWED | Posted: 31 August 2022 doi:10.20944/preprints202011.0700.v4

Table 2: Analytical Model Parameters

	Bacteriorhodopsin	Anoxygenic RC
Y (protons / cycle)	1	2
V_{max} (cycles / second)	100	150
k (kDa)	26	150
b (Å^2)	0.982	2.392
a (Å^2 kDa^{-1})	0.163	0.163
D (photon^{-1})	$1.6 \cdot 10^{-6}$	$1.6 \cdot 10^{-6}$
R (s^{-1})	$2.78 \cdot 10^{-5}$	$2.78 \cdot 10^{-5}$

Variables used for analytical model of phototrophy. See supplement S2 for calculation of these variables from a review of relevant literature.

The behavior of this model follows Michaelis–Menten kinetics with regards to light absorption by its pigment cross-section and its conversion by the catalytic core - see equations S5-S10 for a detailed description of this behavior. Both the antenna and the core are also subject to photodegradation. We modified the methods of Faizi et al., 2018[83] to determine the rate of photodegradation of the phototrophic machinery at different light intensities. By combining this rate of photodegradation with a rate of dilution of degraded protein by growth and dilution/recycling[84], we derived the fraction of functional protein - see equations S11-S14. By applying this photodegradation and dilution correction to the flux of energy through the catalytic core, we arrive at equation 5 (see supplemental equation S15) and equation 6 (see supplemental equation S16) describing the flux per unit protein F_p (protons per kilodalton per second) and the flux per unit incident light F_L (protons per kDa per second per micromole of photons per square meter per second) of a phototrophic system.

Equation 5:

$$F_p = \frac{Y \cdot L \cdot V_{\max} \cdot (ax+b)}{(k+x) \cdot (V_{\max} + L \cdot (ax+b))} \cdot \frac{R}{R + \frac{D \cdot L^2 \cdot (ax+b)^2}{V_{\max} + L \cdot (ax+b)}}$$

Equation 6:

$$F_L = \frac{Y \cdot V_{\max} \cdot (ax+b)}{(k+x) \cdot (V_{\max} + L \cdot (ax+b))} \cdot \frac{R}{R + \frac{D \cdot L^2 \cdot (ax+b)^2}{V_{\max} + L \cdot (ax+b)}}$$

We varied light intensity L the model was exposed to from 0.01 to 4000 micromoles of photons per square meter per second (the upper range is similar to the radiation intensity of full sun at the equator). At each light intensity, we numerically optimized the chlorophototrophic and retinalophototrophic model to determine the quantity of antenna x required to maximize energy flux per unit mass. The mass of antenna complexes associated with each catalytic core were allowed to vary freely, reflecting the widely varying stoichiometry of antennas to reaction centers observed

Preprints (www.preprints.org) | NOT PEER-REVIEWED | Posted: 31 August 2022 doi:10.20944/preprints202011.0700.v4

across the tree of life. We calculated this optimal flux per unit protein F_p and energy flux per unit light F_L for these optimized systems at all light intensities. We then plotted the efficiency per unit incident light and efficiency per unit protein infrastructure of optimal chlorophototrophs and retinalophototrophs at all light intensities.

We find that for both chlorophototrophs and retinalophototrophs, the optimal quantity of antenna per functional unit drops rapidly with increasing light intensity, with no upper limit at arbitrarily low light levels and reaching zero antenna or as low as 2 kDa of antenna at the highest light intensities for chlorophototrophs and retinalophototrophs respectively. Efficiency per unit incident light falls nonlinearly as light intensity increases due to both saturation of the central catalytic core, and drastic decreases in optimal antenna quantity (see supplemental figure 2). Efficiency per unit protein machinery, conversely, rises nonlinearly as light intensity increases due to increased utilization of the catalytic core and a smaller antenna mass, with chlorophototrophs exhibiting a slightly decreased efficiency at the highest light intensities due to photodegradation. Importantly, with the parameters used in our analysis there exists a clear crossover point of $\sim$186 micromoles of photons per square meter per second, above which retinalophototrophy is superior to chlorophototrophy in both measures (Figure 6A-B). In this environment, both the energy flux per unit infrastructure and energy flux per unit incident light are superior for retinalophototrophs. Below this light intensity, chlorophototrophy dominates for both metrics. Light intensity thus determines which phototrophic system will be more efficient.

Notably, while optimal antenna mass increases without limit at low light levels, we calculate a theoretical minimum optimal antenna mass of approximately 95 kDa for chlorophototrophs at the crossover point light level (supplemental figure 2). The lower chlorophototrophic antenna limit is only approximately 20% smaller than the mass of the smallest intrinsic antennas observed in nature in type I reaction centers[43]. While we calculate a maximum antenna size of 61 kDa for antennas associated with rhodopsins at the crossover point, this predicted mass is below the mass of any observed antenna complex and rapidly falls to negligible mass as light intensity increases towards full sunlight. In addition to this, the crossover point at which higher light intensities are dominated by retinalophototrophy corresponds closely with the empirically observed light intensity above which retinal is over-represented in the ocean and chlorophyll is under-represented[52] (see supplement S2 and supplemental figure 5). Our simple model thus recapitulates key physiological trade-offs underlying variation in phototrophic niche space, able to correctly predict the environmental conditions under which either chlorophototrophs or retinalophototrophs should have a physiological and ecological advantage.

4 Discussion

Phototrophic niche partitioning

Phototrophic organisms face a fundamental trade-off between efficiency per unit light and flux per unit infrastructure. The two photosystems that have evolved on Earth each have optimized a different side of this trade-off, profoundly impacting their physiology and ecology. Chlorophototrophy, with a lower energy flux per unit infrastructure, requires a significant fraction of the proteome to be invested to result in an effective energy flux, and is the only phototrophic pathway observed in obligate phototrophs[85,86]. Retinalophototrophy, with its high energy flux per unit infrastructure but

Preprints (www.preprints.org) | NOT PEER-REVIEWED | Posted: 31 August 2022 doi:10.20944/preprints202011.0700.v4

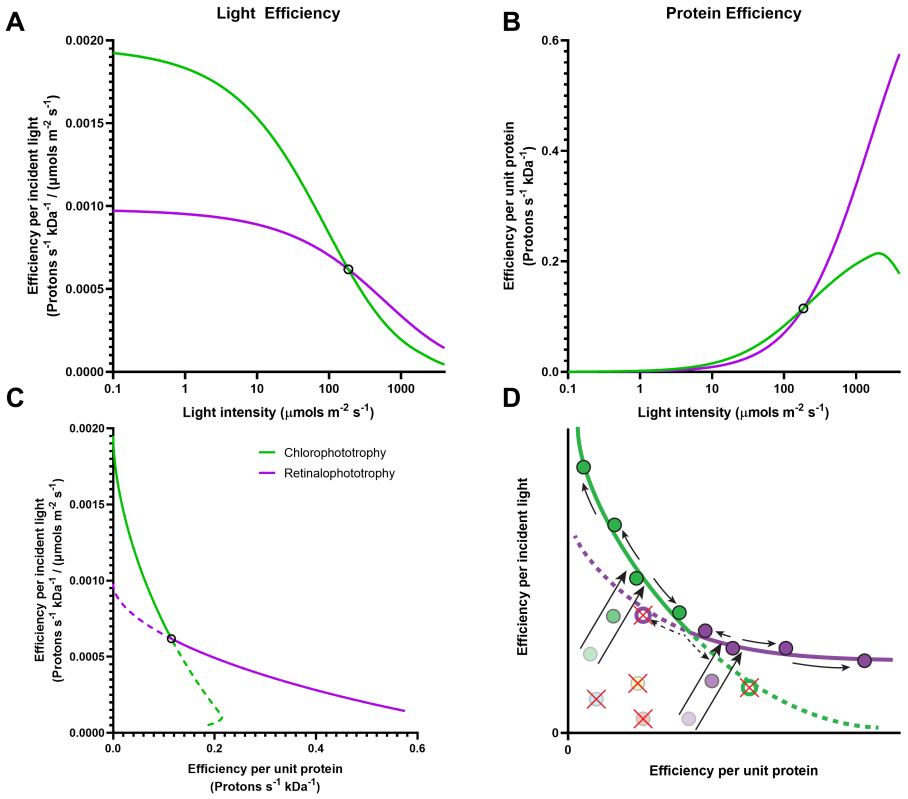

Figure 6: **Fundamental trade-offs in phototrophic machinery dictate ecological interactions and evolutionary trajectories. A)** Results of modeling efficiency per unit incident light for optimal chlorophototrophs (green) and retinalophototrophs (purple). **B)** Results of modeling efficiency per unit protein infrastructure for optimal chlorophototrophs and retinalophototrophs. **C)** Plot of efficiency per unit incident light versus efficiency per unit protein for all light intensities. Each phototrophic system defines overlapping 'Pareto fronts' in this space, on which a system must sit to compete in today's biosphere. These curves cross, indicating that in some ecological niches one system or the other is optimal (solid lines) or non-competitive (dotted lines). **D)** Schematic illustration of hypothesized evolutionary history of phototrophic metabolism on Earth. All modern chlorophototrophs (dark green circles) and retinalophototrophs (dark purple diamonds) lay roughly along their respective Pareto fronts representing a trade-off between energy captured per incident photon and wattage available per unit phototrophic infrastructure. Early chlorophototrophs (light green circles) and retinalophototrophs (light purple circles) lay far away from this Pareto front, and rapidly evolved towards it, subsequently diversifying along the front (arrows). Each phototrophic metabolism suppresses the evolution of novel unrelated phototrophic pathways that are ecologically similar to it but strictly inferior in their initial, unoptimized forms as well as the evolution of forms of the other dominant metabolism that cannot compete in a given ecological niche (red Xs).

Preprints (www.preprints.org) | NOT PEER-REVIEWED | Posted: 31 August 2022 doi:10.20944/preprints202011.0700.v4

lower yield, is broadly distributed across the tree of life (e.g., it is found in 50% of bacteria in the open ocean[58,77,87], heterotrophic protists[55,56] and fungi[60,88], and even as a supplementary system in chlorophototrophic diatoms[89] and basal cyanobacteria). As a pathway with a higher flux per unit protein, it can provide a benefit in high light with less total protein expression, allowing it to be used as a backstop to prevent starvation and increase metabolic flexibility and biomass yield of otherwise heterotrophic organisms without specialization [52,90,91].

These differences stem from an intrinsic biophysical trade-off. Chlorophototrophy's outsized benefits at low light intensity come from its ability to extract twice the energy of a photon as a retinalophototroph. In the low light limit where the mass of an optimal phototrophic system is dominated by antenna complexes, the differing mass of the core catalytic complexes is a minor contributor. As light intensity increases and the optimal phototrophic system requires less and less antenna complex, the lower maximum energy flux per unit mass of the large chlorophototrophic reaction center compared to a rhodopsin begins to dominate and the larger absorption cross section of the reaction center makes it more vulnerable to photodegradation. Both of these differences likely originate from the need for the more efficient reaction center to be large enough to coordinate multiple interacting redox cofactors in order to perform efficient redox chemistry, compared to the simple rhodopsin's single relatively inefficient isomerizing pigment.

A similar trade-off between rate per unit infrastructure and yield has been found in heterotrophic metabolism. The difference between respiration and fermentation itself is a prime example - respiration can produce several times the ATP per unit substrate consumed while producing less than half the energy flux per unit protein mass[92]. The two most common glycolytic pathways - the Etner-Doudoroff (ED) and Embden-Meyerhof-Parnas (EMP) pathway - share precisely this relationship as well. The EMP pathway produces twice the ATP per unit carbohydrate consumed as the ED pathway, but requires 5 times as much protein, and thus produces approximately 40% the energy flux per kilodalton of protein[93]. Much like obligate phototrophs, which exclusively use the high efficiency strategy of chlorophotorophy, obligate anaerobes tend to use the the EMP pathway, which similarly makes more efficient use of their substrate but come with a larger investment in protein infrastructure.

Differences in the cost of metabolic machinery have major implications for growth and ecology. The larger the fraction of a cell's proteome that must be put towards the generation and maintenance of energy and resources, the smaller the fraction of the proteome can go towards growth and development[94]. This leads to a series of 'growth laws'[95,96] which dictate that, all else being equal, a larger investment of protein being used to efficiently consume a rare resource leads to a slower growth rate due to less investment in new ribosomes and anabolic functions. The optimal allocation of costly metabolic enzymes under situations of differing growth rate and resource availability therefore explains much of the long-observed trade-off between microbial growth rate and biomass yield[92,94,96,97]. Rapid growth and low yield occurs on abundant resources, while slow growth and high yield occurs on scarce resources. Only recently has optimal proteome allocation been analyzed in the context of phototrophy and autotrophy in general[83,98,99], but the principles are identical when ambient light is treated as a metabolic resource.

Chlorophototrophy and retinalophototrophy thus have partitioned phototrophic niche space. Chlorophototrophy is a high-investment strategy suitable for environments of low growth rate, low

Preprints (www.preprints.org) | NOT PEER-REVIEWED | Posted: 31 August 2022 doi:10.20944/preprints202011.0700.v4

ambient light resources, or for specialists investing heavily in a single pathway regardless of their environment environment (i.e., obligate photoautotrophs). Retinalophototrophy is a low-investment strategy suitable for situations of higher growth rate, high ambient light resources, or for flexible metabolic generalists capable of both phototrophy and heterotrophic metabolism. Taken together with other divergent properties including chlorophototrophy's requirement of potentially growth-limiting iron and the ease of horizontal transfer of retinalophototrophic capacity over evolutionary time, the properties of these two phototrophic pathways are strikingly complementary.

Ecological interference, evolutionary priority effects, and major evolutionary innovations

The ecologically complementary nature of Earth's two phototrophic systems suggests that their properties have co-evolved, rather than their properties being independent of each other's existence. In particular, we propose that the evolution of phototrophy has been shaped by the phenomenon of evolutionary priority effects. Much like an ecological priority effect in which the first organisms to colonize a habitat become difficult to displace[100,101], an evolutionary priority effect is a process by which a poorly-adapted newcomer evolves into a new ecological niche, suppressing the evolution of similar newcomers which could fill the same niche[101–103].

Each extreme of the efficiency per unit investment / efficiency per unit light trade-off represents a different emergent phototrophic niche. The set of optimal machineries for a given situation represents a Pareto front on a plot of these two variables against each other[104,105] (Figure 6C). Natural selection should move phototrophic systems towards this front from any suboptimal starting point. Once the Pareto front has been reached, increasing efficiency along one axis requires decreasing it along the other axis, and subsequent adaptation should largely be occur along this curve. Each phototrophic machinery type exhibits its own Pareto front, the point at which they cross indicates how variation in light intensity creates distinct niches in which either photosystem will be superior.

Fundamental architectural limitations of the catalytic cores of each phototrophic system ensure that the extremes of the investment / resource efficiency tradeoff are only accessible to one or the other. Microbial rhodopsins are a small, light-driven proton pump driven by isomerization of a single small molecule, which only allows a single proton to be pumped per photocycle[50]. It would be difficult, if not impossible, for it to be reworked into a more efficient form without a complete restructuring. Without any redox-active cofactors in its structure, it cannot be recruited to interact with electron transport chains or redox metabolism. Rhodopsin thus appears to be incapable of evolving to pump more than one proton per photon and efficiently using available light resources, although its small mass means it enjoys a high maximum energy flux per unit mass. Conversely, the mass of the core machinery of the chlorophototrophic reaction center appears to be constrained such that it cannot be reduced below a relatively large minimum size. While proteobacterial type II RCs have either lost or never acquired the integrated antenna domains common to other RCs[53], the core catalytic subunit appears to never mass under approximately 150 kilodaltons[30] or contain fewer than a minimum of eight cofactor molecules[30,31]. This minimal unit likely cannot be shrunk further while retaining its function in redox metabolism, limiting its maximum energy flux per unit mass even as it enjoys a high efficiency per unit light captured.

Today, this means that chlorophototrophy and retinalophototrophy are ecologically partitioned towards one or another end of the trade-off between energy flux per unit protein investment and

energy flux per unit light. Together, they continue to engender an evolutionary priority effect preventing any other rudimentary phototrophic systems from becoming established (Figure 6D), maintaining this dual singularity. All modern phototrophs will exist somewhere along the combined Pareto front embodied by the trade-of curves of each system, and any newly-evolved phototrophic system will inevitably be slow, inefficient, and generally poorly adapted compared to these well-established systems. Incapable of invading resident phototrophs, evolutionary priority effects would limit phototrophy to these two systems, even if, in principle, the evolution of novel photosysems is easy.

According to this view of evolutionary priority effects, whichever pathway evolved first would have rapidly improved itself until it ran into physical limitations and began exploring its own Pareto front. Why didn't the first mover diversify to fill both low and high-light niches, resulting in a true evolutionary singularity? The answer may lie in the fact that, while chlorophototrophs are able to use light energy for either pumping protons via an electron transport chain for energy or reduction of CO_2 into biomass, retinalophototrophs are only capable of using light for energy. They are fundamentally incapable of driving redox reactions directly and fail to push the membrane to a high enough voltage to counteract electron transport chains, a precondition for driving carbon fixation via reverse electron flow[51]. This means that there is, effectively, a third dimension to the ecological niche of phototrophy representing the ability to fix carbon using light energy. Assuming that the earliest chlorophototrophs engaged in redox chemistry[23], even a slow and poorly adapted proto-chlorophototroph would be superior to a retinalophototroph in its ability to fix carbon away from geologically provisioned electron sources. This would allow a way around the priority effect engendered by an established retinalophototroph, and an opportunity to evolve until it too became well-established and filled its own area of the trade-off curve (Figure 6D).

If this model is correct, the fact that a second ecologically-complementary phototrophic pathway evolved suggests that the origin of novel phototrophic systems is not necessarily a low-probability, evolutionarily-difficult innovation. Instead, it suggests that early forays into phototrophy may have occurred many times in the history of life. All but two of these novel, unoptimized pathways would simply have been driven to extinction by competition with the well-adapted first-movers. Furthermore, this model implies that retinalophototrophy likely evolved before chlorophototrophy, given that carbon fixation allows a proto-chlorophototroph to avoid evolutionary priority effects from retinalophototrophs but not the opposite. This implication fits with the known properties of the two systems. Retinalophototrophy is much simpler than chlorophototrophy in terms of genes required, and while a microbial rhodopsin is useful in any organism that uses a proton gradient across a membrane, chlorophototrophic machinery is itself part of a much larger electron transport chain and has many more prerequisites.

Evidence for ancient suppressed major innovations

Understanding the origins of evolutionary innovations that occurred billions of years ago poses considerable challenges. Surviving phototrophic pathways do not bear direct evidence of evolutionary priority effects in their structures, but instead only suggest it in their relationship to each other. The extinction of prospective newcomers after niches are filled makes it difficult to directly test the hypothesis that additional phototrophic pathways could have emerged but have

Preprints (www.preprints.org) | NOT PEER-REVIEWED | Posted: 31 August 2022 doi:10.20944/preprints202011.0700.v4

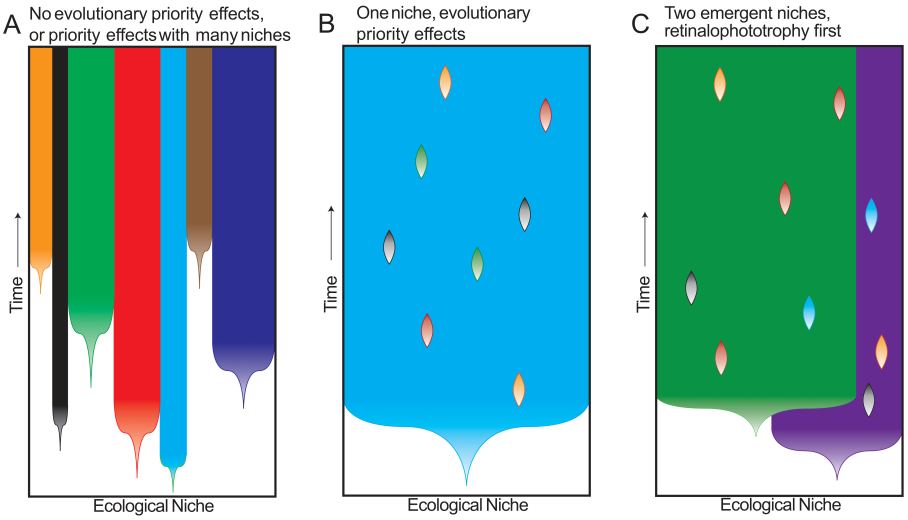

Figure 7: **Evolutionary priority effects and their impact on major evolutionary innovations. A)** The filling of ecological niches in a system with low evolutionary priority effects. A large number of separate innovations fill separate niches. This model roughly describes the multiple origins of complex multicellularity. **B)** Hypothesized circumstance of evolutionary priority effects maintaining the appearance of an 'evolutionary singularity' - a single innovation can fill all available niches of a given type, and continually outcompetes novel innovators. The singular origin of life and eukaryogenesis could be represented by this model. **C)** Our inferred model of the history of the evolution of phototrophy on Earth. As chlorophototrophy could likely suppress the *de novo* evolution of retinalophototrophy, but not the opposite, retinalophototrophy likely came first but was driven out of high efficiency per unit light niches by well-adapted chlorophototrophs once they were evolutionarily mature. For most of the history of life on Earth, the two together have suppressed the evolution of novel phototrophic systems, each filling their respective sides of the efficiency per unit investment / efficiency per unit substrate Pareto front.

Preprints (www.preprints.org) | NOT PEER-REVIEWED | Posted: 31 August 2022 doi:10.20944/preprints202011.0700.v4

been suppressed through competition. However, direct evidence of independently originating light-harvesting pathways which have not been refined into niche-defining and biosphere-changing metabolic pathways may survive to the present day in the form of light-driven processes that are not involved directly in energy metabolism. Specifically, they may be preserved if they are co-opted for some ancillary purpose unconnected to any particular phototrophic niche, and thus provide a selective advantage while not competing with entrenched phototrophic metabolisms. Such preserved pathways would likely be comparatively unoptimized, using generic cofactors rather than dedicated pigment molecules, as they have not been subject to the strong selection present when a significant metabolic flux passes through a specialized pathway.

Two modern pathways are of particular interest in their similarity to this template. The most well-studied is DNA repair mediated by photolyases, using light energy to repair pyrimidine dimers created by ultraviolet radiation[106]. A second, more recently discovered class of proteins known as fatty acid photodecarboxylases also use light energy for the production of hydrocarbon oils in algae in a similar way[107]. Their mechanism of operation resembles that of chlorophototrophic reaction centers, while being composed of non-homologous components. The active site of both of these proteins contains FAD - a redox cofactor, which happens to absorb and interact with light incidental to its main function as an electron carrier due to its large set of fused aromatic rings. Held nearby in the enzyme is an additional molecule of MTHF (5,10-methenyltetrahydrofolate, a cofactor involved in methyl group metabolism) or 8-HDF (8-hydroxy-5-deazaflavin, a molecule related to other flavins), both of which also happen to be incidentally photoactive. But in photolyases and fatty acid decarboxylases, rather than performing any methyl-group chemistry or redox chemistry, the large absorption cross section for visible light of both of these is instead exapted. They function as an antenna pigment, absorbing photons that would not be absorbed by FAD, and transferring this energy into the FAD and exciting it[106,108]. Once excited, FAD then transfers an electron to the substrate and reduces it, transiently becoming an oxidizing agent and a radical stabilized by the apoprotein[106–108]. This electron triggers a rearrangement of bonds in the substrate, repairing a pyrimidine dimer or decarboxylating a fatty acid, before returning to the oxidized FAD in a form of localized circular electron flow.

Thus, photolyases and fatty acid photodecarboxylases contain repurposed ordinary metabolic and redox cofactors which happen to be photoactive independent of their primary functions. They contain cofactors acting as antenna pigments, transferring excitations into redox-active cofactors at active sites of proteins, analogous to the light-gathering chlorophylls and central redox-active chlorophylls of chlorophototrophic reaction centers. Both drive a form of circular electron flow, much as chlorophototrophic reaction centers drive circular electron transport chains to capture biological energy. Their similarities to photosynthetic machinery have been noticed by numerous authors in the astrobiological literature, and used as proof of concept for alternate phototrophic metabolisms that never came to be on Earth[108,109]. It is not difficult to imagine how these light-transducing systems could become more optimized over evolutionary time, with customization of FAD and MTHF into dedicated phototrophic pigments and their electron flow being directed into electron transport chains and redox metabolism for carbon fixation. And yet they never were, and we instead observe this unique bit of photochemistry pushed to the margins of metabolism, directly driving DNA repair and other metabolic reactions that require a small, local circular

Preprints (www.preprints.org) | NOT PEER-REVIEWED | Posted: 31 August 2022 doi:10.20944/preprints202011.0700.v4

electron flow rather than a globally available reducing agent or energy carrier. These two apparently independent reactions are precisely what would be expected of a remnant of separate origins of prospective phototrophic metabolism if it were to survive by being applied to a purpose independent of phototrophy, and provide evidence for the existence of an alternate evolvable phototrophic metabolism that has been driven to the margins by incumbents.

These ancillary photoactive pathways may recapitulate something of the nature of the earliest phototrophic systems, before they were optimized and became capable of suppressing newcomers. While the nature of the earliest retinalophototrophic machinery is somewhat mysterious, as the small protein's limited structural homology with anything except eukaryotic G-protein coupled receptors and sensory rhodopsins restricts inferences of their early evolution[20,110], the nature of the earliest precursors of chlorophototrophy are relatively well constrained. Several main structural attributes of the last common ancestor of the reaction center complex can be inferred[32,43,111,112]. All reaction centers contain three central pairs of carefully coordinated chlorophyll or bacteriochlorophyll molecules that when excited are able to trigger electron transfer, as well as additional pigment molecules both in the reaction center itself and in associated antenna pigments transferring their energy to the redox-active catalytic center. This combination of a redox-active central complex plus antennas seems to be ancient. It has also been clear for decades that chlorophyll is evolutionarily related to tetrapyrroles such as heme[23,113,114]. Heme is a redox cofactor, binding iron to carry electrons through electron transport chains or perform catalysis in enzymes (its role in binding oxygen in animal globins being a late, derived function). Thus, the chlorophototrophic system is likely ultimately derived from a modified respiratory electron transport chain component[23,115]. Heme already is mildly photoactive much like flavins and MTHF. It absorbs ultraviolet and short-wavelength visible light, though this usually results in destruction of the molecule[116,117]. Synthesis of chlorophyll involves the modification of the common tetrapyrrole backbone and insertion of a different bound ion which tunes its absorption features further into the visible light range and its available excited states into those which can reversibly transfer electrons. Many scenarios have been proposed for the details the evolution of this process[23]. Ultimately heme or another tetrapyrrole was likely optimized into a dedicated pigment over evolutionary time, in the context of an electron transport chain driven by external redox couples that came to be able to rely on internal generation of redox power.

Evolutionary priority effects may play a role in other singular innovations

More generally, our results imply that the evolution of many singular innovations may be less difficult than they appear. Easily accessible innovations can be preserved for long periods of time as apparent singularities or near-singularities when evolutionary priority effects strongly inhibit subsequent innovation. The extent to which evolutionary priority effects can constrain subsequent innovation depends on the underlying 'niche structure'. In the absence of either competition or evolutionary priority effects, innovations are not suppressed and are free to evolve repeatedly. Multicellularity, for example, has evolved many times[1], allowing for fundamentally different multicellular life history strategies to evolve in different lineages (as in Figure 7A). The evolution of fungi does not seem to constrain the evolution of plants or animals, for instance. In contrast, singularities are expected when there is a singular broad niche and no strict architectural limitations like those which have emergently prevented chlorophototrophs or retinalophototrophs from evolving

Preprints (www.preprints.org) | NOT PEER-REVIEWED | Posted: 31 August 2022 doi:10.20944/preprints202011.0700.v4

to dominate all phototrophic niches (Figure 7B). Life itself, an ancient singularity, may in a sense occupy a single broad niche in which powerful evolutionary priority effects suppress secondary origins of inefficient and simple novel replicators and protocells. The evolution of eukaryotes, another singularity of profound importance, could represent a similar case of a newcomer inventing a transformative capability - most likely phagocytosis or other capacities for complex and flexible cell morphology[118] - and subsequently suppressing secondary origins. The dual singularity of phototrophy (Figure 7C) thus represents a special case of a large, open ecological niche with just sufficient structure and architectural limitations in the first-movers to prevent the maintenance of a true singularity, revealing the role of evolutionary priority effects and ecological interactions to careful investigation.

Marginalized secondary origins of major evolutionary innovations that can reveal the existence of evolutionary priority effects may not be unique to the evolution of phototrophy. Eukaryogenesis has long been considered a classical evolutionary singularity, unique in its origin of complex cell architectures. However with the discovery of the Asgard archaea, a clade bearing many features previously believed to be specific to eukaryotes[119] including functional cytoskeletal components[120] ribosomal RNA expansions[121] and even SNARE proteins associated with endomembrane systems[122], the uniqueness of eukaryotes has been cast into doubt. Recently, a striking example of a separate invention of complex cellular architecture has been discovered - a subset of planctomycete bacteria which possesses a phagotrophic lifestyle, consuming other bacteria in a manner previously thought to be unique to eukaryotes[123]. This bacterial group has long been known for large size and an unusually complex if poorly understood cellular architecture[124,125] and has convergently evolved a proteome uniquely rich in gene duplications and large multidomain proteins for a bacterium[126], qualitatively similar to those of simple eukaryotes.

Does the evolution of this phagotrophic bacterium represent an independent invention of complex cell architecture and increased genetic complexity analogous to eukaryogenesis, and if so what could have protected it from priority effects from incumbent eukaryotes in its unique ecological niche? One possibility is metabolic niche partitioning. Planctomycete bacteria are known for having remarkably specialized metabolisms, including the anammox reaction[127]. Eukaryotes are notoriously limited in their metabolic repertoire compared to bacteria, instead relying on size and morphological complexity for adaptation to new niches[118]. One possibility is that a highly specialized metabolic niche could have protected this lineage from competition with eukaryotes, allowing them to evade suppression by evolutionary priority effects and evolve eukaryote-like cellular properties until able to compete with eukaryotes outside their protected environment.

5 Conclusion

Phototrophy is among the most important innovations in the history of life, fundamentally changing the biosphere. It is unique among major biological innovations in that it has evolved not once, and not many times, but exactly twice. Here we show that the two origins of phototrophy are mechanistically and ecologically complementary, having partitioned phototrophic niche space along a set of trade-offs that prevent either mechanism from becoming dominant.

Architectural limitations and functional trade-offs inherent to each type of phototrophy appear to have prevented either chlorophototrophs or retinalophototrophs from occupying every

phototrophic niche, creating the opportunity for the stable coexistence of both pathways. The fact that phototrophy has evolved just two times over the history of Earth's biosphere, particularly given the existence of alternative pathways capable of generating energy from light, suggests that additional independent origins have been suppressed by evolutionary priority effects once every niche was effectively filled. We are not the first to argue that priority effects could lead to evolutionary singularities[21], but until now, it has been impossible to disentangle this hypothesis from the possibility that most impactful singularities exist because they are in some way fundamentally evolutionarily difficult.

The origin of major evolutionary innovations cannot be understood outside of their ecological and evolutionary contexts. Fundamental questions still remain unresolved: how pervasive is evolutionary suppression due to evolutionary priority effects? What determines a new innovation's niche structure? Within the same niche, does competitive exclusion always occur? Three lines of future work stand to be especially informative: First, we should integrate theoretical and empirical approaches to understand the conditions under which evolutionary priority effects constrain innovation. Second, we should make use of Earth's natural experiments, comparing the innovations that have occurred repeatedly (e.g., multicellularity, super-organismality, C4 photosynthesis) to those that have occurred just once or twice (e.g., phototrophy, eukaryogenesis). Finally, we should search for undiscovered vestiges of independent innovations that have survived either by alleviating evolutionary priority effects or by having their function modified to avoid competition with the 'primary' innovation. Together, this work stands to provide significant insight into the nature of evolutionary innovations and the origin of complex life.

1. Herron, M. D., Rashidi, A., Shelton, D. E. & Driscoll, W. W. Cellular differentiation and individuality in the 'minor' multicellular taxa. *Biological Reviews* **88**, 844–861 (2013).

2. Knoll, A. H. The Multiple Origins of Complex Multicellularity. *Annual Review of Earth and Planetary Sciences* **39**, 217–239 (2011). URL http://www.annualreviews.org/doi/10.1146/annurev.earth.031208.100209.

3. Nagy, L. G., Kovács, G. M. & Krizsán, K. Complex multicellularity in fungi: evolutionary convergence, single origin, or both? *Biol. Rev* **93**, 1778–1794 (2018).

4. Bengtson, S., Sallstedt, T., Belivanova, V. & Whitehouse, M. Three-dimensional preservation of cellular and subcellular structures suggests 1.6 billion-year-old crown-group red algae. *PLoS Biology* **15**, 1–38 (2017). URL http://dx.doi.org/10.1371/journal.pbio.2000735.

5. Bengtson, S. *et al.* Fungus-like mycelial fossils in 2.4-billion-year-old vesicular basalt. *Nature Ecology and Evolution* **1**, 1–6 (2017). URL http://dx.doi.org/10.1038/s41559-017-0141.

6. El Albani, A. *et al.* The 2.1 Ga old Francevillian biota: Biogenicity, taphonomy and biodiversity. *PLoS ONE* **9** (2014).

7. Smith, J. M. & Szathmary, E. *The major transitions in evolution* (Oxford University Press, 1997).

8. Sage, R. F. The evolution of c4 photosynthesis. *New phytologist* **161**, 341–370 (2004).

9. Alexander, D. E. *On the wing: Insects, pterosaurs, birds, bats and the evolution of animal flight* (Oxford University Press, USA, 2015).

10. Vetsigian, K., Woese, C. & Goldenfeld, N. Collective evolution and the genetic code. *Proc Natl Acad Sci U S A* **103**, 10696–701 %U internal–pdf://vetsigian et al pnas 2 (2006). URL http://www.ncbi.nlm.nih.gov/pubmed/16818880.

11. Esser, C. *et al.* A genome phylogeny for mitochondria among α-proteobacteria and a predominantly eubacterial ancestry of yeast nuclear genes. *Molecular Biology and Evolution* **21**, 1643–1660 (2004).

12. Martijn, J., Vosseberg, J., Guy, L., Offre, P. & Ettema, T. J. Deep mitochondrial origin outside the sampled alphaproteobacteria. *Nature* **557**, 101–105 (2018).

13. Lane, N. Serial endosymbiosis or singular event at the origin of eukaryotes? *Journal of Theoretical Biology* **0**, 1–10 (2017).

14. Lane, N. Bioenergetic constraints on the evolution of complex life. *Cold Spring Harb Perspect Biol* **6**, a015982 (2014).

15. Monod, J. *On Chance and Necessity*, 357–375 (Macmillan Education UK, London, 1974). URL https://doi.org/10.1007/978-1-349-01892-5_20.

16. Walter, M., Buick, R. & Dunlop, J. Stromatolites 3,400–3,500 myr old from the north pole area, western australia. *Nature* **284**, 443–445 (1980).

17. Van Kranendonk, M. J., Philippot, P., Lepot, K., Bodorkos, S. & Pirajno, F. Geological setting of earth's oldest fossils in the ca. 3.5 ga dresser formation, pilbara craton, western australia. *Precambrian Research* **167**, 93–124 (2008).

18. Nutman, A. P., Bennett, V. C., Friend, C. R., Van Kranendonk, M. J. & Chivas, A. R. Rapid emergence of life shown by discovery of 3,700-million-year-old microbial structures. *Nature* **537**, 535–538 (2016).

19. DasSarma, S. & Schwieterman, E. W. Early evolution of purple retinal pigments on earth and implications for exoplanet biosignatures. *International Journal of Astrobiology* 1–10 (2018).

20. Shen, L., Chen, C., Zheng, H. & Jin, L. The evolutionary relationship between microbial rhodopsins and metazoan rhodopsins. *The Scientific World Journal* **2013** (2013).

21. De Duve, C. *Singularities: landmarks on the pathways of life* (Cambridge University Press, 2005).

22. Decker, K., Jungermann, K. & Thauer, R. Energy production in anaerobic organisms. *Angewandte Chemie International Edition in English* **9**, 138–158 (1970).

23. Martin, W. F., Bryant, D. A. & Beatty, J. T. A physiological perspective on the origin and evolution of photosynthesis. *FEMS microbiology reviews* **42**, 205–231 (2018).

24. Lyons, T. W., Reinhard, C. T. & Planavsky, N. J. The rise of oxygen in earth's early ocean and atmosphere. *Nature* **506**, 307–315 (2014).

25. Hazen, R. M. *et al.* Mineral evolution. *American Mineralogist* **93**, 1693–1720 (2008).

26. Bryant, D. A. & Frigaard, N.-U. Prokaryotic photosynthesis and phototrophy illuminated. *Trends in microbiology* **14**, 488–496 (2006).

27. Thiel, V., Tank, M. & Bryant, D. A. Diversity of Chlorophototrophic Bacteria Revealed in the Omics Era. *Annual Review of Plant Biology* **69**, annurev–arplant–042817–040500 (2018). URL http://www.annualreviews.org/doi/10.1146/annurev-arplant-042817-040500.

28. Ward, L. M., Cardona, T. & Holland-Moritz, H. Evolutionary implications of anoxygenic phototrophy in the bacterial phylum candidatus eremiobacterota (wps-2). *Frontiers in microbiology* **10**, 1658 (2019).

29. Field, C. B. Primary Production of the Biosphere: Integrating Terrestrial and Oceanic Components. *Science* **281**, 237–240 (1998). URL http://www.sciencemag.org/cgi/doi/10.1126/science.281.5374.237.1011.1669.

30. Niwa, S. *et al.* Structure of the lh1–rc complex from thermochromatium tepidum at 3.0 å. *Nature* **508**, 228–232 (2014).

31. Noy, D., Moser, C. C. & Dutton, P. L. Design and engineering of photosynthetic light-harvesting and electron transfer using length, time, and energy scales. *Biochimica et Biophysica Acta (BBA)-Bioenergetics* **1757**, 90–105 (2006).

32. Cardona, T. A fresh look at the evolution and diversification of photochemical reaction centers. *Photosynthesis Research* **126**, 111–134 (2015). URL https://doi.org/10.1007/s11120-014-0065-x.

33. He, G., Zhang, H., King, J. D. & Blankenship, R. E. Structural analysis of the homodimeric reaction center complex from the photosynthetic green sulfur bacterium chlorobaculum tepidum. *Biochemistry* **53**, 4924–4930 (2014).

34. Tsukatani, Y., Romberger, S. P., Golbeck, J. H. & Bryant, D. A. Isolation and characterization of homodimeric type-i reaction center complex from candidatus chloracidobacterium thermophilum, an aerobic chlorophototroph. *Journal of Biological Chemistry* **287**, 5720–5732 (2012).

35. Fromme, P., Jordan, P. & Krauß, N. Structure of photosystem i. *Biochimica et Biophysica Acta (BBA)-Bioenergetics* **1507**, 5–31 (2001).

36. He, Z. *et al.* Reaction centers of the thermophilic microaerophile, chloracidobacterium thermophilum (acidobacteria) i: biochemical and biophysical characterization. *Photosynthesis research* **142**, 87–103 (2019).

37. Umena, Y., Kawakami, K., Shen, J.-R. & Kamiya, N. Crystal structure of oxygen-evolving photosystem ii at a resolution of 1.9 å. *Nature* **473**, 55–60 (2011).

38. Nagashima, S. & Nagashima, K. V. Comparison of photosynthesis gene clusters retrieved from total genome sequences of purple bacteria. In *Advances in Botanical Research*, vol. 66, 151–178 (Elsevier, 2013).

39. Xin, Y. *et al.* Cryo-em structure of the rc-lh core complex from an early branching photosynthetic prokaryote. *Nature communications* **9**, 1–10 (2018).

40. Shikanai, T. Chloroplast NDH: A different enzyme with a structure similar to that of respiratory NADH dehydrogenase. *Biochimica et Biophysica Acta - Bioenergetics* **1857**, 1015–1022 (2016). URL http://dx.doi.org/10.1016/j.bbabio.2015.10.013.

41. Zhu, J., Vinothkumar, K. R. & Hirst, J. Structure of mammalian respiratory complex i. *Nature* **536**, 354–358 (2016).

42. Nawrocki, W. *et al.* The mechanism of cyclic electron flow. *Biochimica et Biophysica Acta (BBA)-Bioenergetics* (2019).

43. Gisriel, C. *et al.* Structure of a symmetric photosynthetic reaction center–photosystem. *Science* **357**, 1021–1025 (2017).

44. Yu, L.-J., Kawakami, T., Kimura, Y. & Wang-Otomo, Z.-Y. Structural basis for the unusual qy red-shift and enhanced thermostability of the lh1 complex from thermochromatium tepidum. *Biochemistry* **55**, 6495–6504 (2016).

45. Kouyianou, K. *et al.* The chlorosome of chlorobaculum tepidum: size, mass and protein composition revealed by electron microscopy, dynamic light scattering and mass spectrometry-driven proteomics. *Proteomics* **11 14**, 2867–80 (2011).

46. Bryant, D. A. & Canniffe, D. P. How nature designs light-harvesting antenna systems: design principles and functional realization in chlorophototrophic prokaryotes. *Journal of Physics B: Atomic, Molecular and Optical Physics* **51**, 033001 (2018).

47. Oesterhelt, D. & Stoeckenius, W. Rhodopsin-like protein from the purple membrane of halobacterium halobium. *Nature new biology* **233**, 149–152 (1971).

48. Sabehi, G. *et al.* New insights into metabolic properties of marine bacteria encoding proteorhodopsins. *PLOS Biology* **3** (2005). URL `https://doi.org/10.1371/journal.pbio.0030273`.

49. Balashov, S. P. *et al.* Xanthorhodopsin: the Retinal Protein Proton Pump of Salinibacter ruber with a Light-harvesting Carotenoid Antenna. *Science (New York, N.Y.)* **309**, 2061–2064 (2005). URL `http://www.ncbi.nlm.nih.gov/pmc/articles/PMC3065861/`.

50. Ernst, O. P. *et al.* Microbial and animal rhodopsins: structures, functions, and molecular mechanisms. *Chemical reviews* **114**, 126–163 (2014).

51. Walter, J. M., Greenfield, D., Bustamante, C. & Liphardt, J. Light-powering Escherichia coli with proteorhodopsin. *Proceedings of the National Academy of Sciences* **104**, 2408–2412 (2007). URL `http://www.pnas.org/cgi/doi/10.1073/pnas.0611035104`.

52. Gómez-Consarnau, L. *et al.* Microbial rhodopsins are major contributors to the solar energy captured in the sea. *Science advances* **5**, eaaw8855 (2019).

53. Cardona, T. Thinking twice about the evolution of photosynthesis. *Open biology* **9**, 180246 (2019).

54. Slamovits, C. H., Okamoto, N., Burri, L., James, E. R. & Keeling, P. J. A bacterial proteorhodopsin proton pump in marine eukaryotes. *Nature Communications* **2**, 183–186 (2011). URL `http://dx.doi.org/10.1038/ncomms1188`.

55. Vader, A., Laughinghouse, H. D., Griffiths, C., Jakobsen, K. S. & Gabrielsen, T. M. Proton-pumping rhodopsins are abundantly expressed by microbial eukaryotes in a high-Arctic fjord. *Environmental Microbiology* **20**, 890–902 (2018).

56. Labarre, A., Obiol, A., Wilken, S., Forn, I. & Massana, R. Expression of genes involved in phagocytosis in uncultured heterotrophic flagellates. *Limnology and Oceanography* **65**, S149–S160 (2020).

57. Sharma, A. K., Spudich, J. L. & Doolittle, W. F. Microbial rhodopsins: functional versatility and genetic mobility. *Trends in Microbiology* **14**, 463–469 (2006).

58. Finkel, O. M., Béjà, O. & Belkin, S. Global abundance of microbial rhodopsins. *ISME Journal* **7**, 448–451 (2013).

59. Nowicka, B. & Kruk, J. Powered by light: Phototrophy and photosynthesis in prokaryotes and its evolution. *Microbiological Research* **186-187**, 99–118 (2016).

60. Gleason, F. H., Larkum, A. W., Raven, J. A., Manohar, C. S. & Lilje, O. Ecological implications of recently discovered and poorly studied sources of energy for the growth of true fungi especially in extreme environments. *Fungal ecology* **39**, 380–387 (2019).

61. Rinke, C. *et al.* A phylogenomic and ecological analysis of the globally abundant Marine Group II archaea (Ca. Poseidoniales ord. nov.). *The ISME Journal* 1 (2018). URL `http://www.nature.com/articles/s41396-018-0282-y`.

62. Sabehi, G. *et al.* New insights into metabolic properties of marine bacteria encoding proteorhodopsins. *PLoS Biology* **3** (2005).

63. Pinhassi, J., DeLong, E. F., Béjà, O., González, J. M. & Pedrós-Alió, C. Marine Bacterial and Archaeal Ion-Pumping Rhodopsins: Genetic Diversity, Physiology, and Ecology. *Microbiology and Molecular Biology Reviews* **80**, 929–954 (2016). URL `http://mmbr.asm.org/lookup/doi/10.1128/MMBR.00003-16`.

64. Brinkmann, H., Göker, M., Koblížek, M., Wagner-Döbler, I. & Petersen, J. Horizontal operon transfer, plasmids, and the evolution of photosynthesis in rhodobacteraceae. *The ISME journal* **12**, 1994–2010 (2018).

65. Umena, Y., Kawakami, K., Shen, J. R. & Kamiya, N. Crystal structure of oxygen-evolving photosystem II at a resolution of 1.9Å. *Nature* **473**, 55–60 (2011). URL `http://dx.doi.org/10.1038/nature09913`.

66. Béjà, O. *et al.* Bacterial Rhodopsin : Evidence for a New Type of Phototrophy in the Sea Bacterial Rhodopsin : Evidence for a New Type of Phototrophy in the Sea. *Science* **289**, 1902–1906 (2000).

67. Zhang, J. *et al.* Structure of phycobilisome from the red alga Griffithsia pacifica. *Nature Publishing Group* **551**, 57–63 (2017). URL `http://dx.doi.org/10.1038/nature24278`.

68. Cunningham, F. X., Dennenberg, R. J., Mustardy, L., Jursinic, P. a. & Gantt, E. Stoichiometry of Photosystem I, Photosystem II, and Phycobilisomes in the Red Alga Porphyridium cruentum as a Function of Growth Irradiance. *Plant physiology* **91**, 1179–1187 (1989).

69. Singharoy, A. *et al.* Atoms to phenotypes: Molecular design principles of cellular energy metabolism. *Cell* **179**, 1098–1111 (2019).

70. Muench, S. P., Trinick, J. & Harrison, M. A. Structural divergence of the rotary atpases. *Quarterly reviews of biophysics* **44**, 311–356 (2011).

71. Scheuring, S. & Sturgis, J. N. Atomic force microscopy of the bacterial photosynthetic apparatus: Plain pictures of an elaborate machinery. *Photosynthesis Research* **102**, 197–211 (2009).

72. Cherezov, V., Clogston, J., Papiz, M. Z. & Caffrey, M. Room to move: Crystallizing membrane proteins in swollen lipidic mesophases. *Journal of Molecular Biology* **357**, 1605–1618 (2006).

73. Herzen, V. *et al.* Bacterial photosynthesis in surface waters of the open ocean. *Nature* **407**, 177–179 (2000).

74. Lubner, C. E. *et al.* Solar hydrogen-producing bionanodevice outperforms natural photosynthesis. *Proceedings of the National Academy of Sciences* **108**, 20988–20991 (2011).

75. Friedrich, T. *et al.* Proteorhodopsin is a light-driven proton pump with variable vectoriality. *Journal of Molecular Biology* **321**, 821 – 838 (2002). URL `http://www.sciencedirect.com/science/article/pii/S0022283602006964`.

76. Lanyi, J. K. Proton transfers in the bacteriorhodopsin photocycle. *Biochimica et Biophysica Acta - Bioenergetics* **1757**, 1012–1018 (2006).

77. Kirchman, D. L. & Hanson, T. E. Bioenergetics of photoheterotrophic bacteria in the oceans. *Environmental Microbiology Reports* **5**, 188–199 (2013).

78. Sener, M., Strumpfer, J., Singharoy, A., Hunter, C. N. & Schulten, K. Overall energy conversion efficiency of a photosynthetic vesicle. *eLife* **5**, 1–30 (2016).

79. Kimura, Y. *et al.* Surface of bacteriorhodopsin revealed by high-resolution electron crystallography. *Nature* **389**, 206–211 (1997).

80. Tomasello, G., Armenia, I. & Molla, G. The protein imager: a full-featured online molecular viewer interface with server-side hq-rendering capabilities. *Bioinformatics* **36**, 2909–2911 (2020).

81. Lanyi, J. K. Proton transfers in the bacteriorhodopsin photocycle. *Biochimica et Biophysica Acta (BBA)-Bioenergetics* **1757**, 1012–1018 (2006).

82. Cherezov, V., Clogston, J., Papiz, M. Z. & Caffrey, M. Room to move: crystallizing membrane proteins in swollen lipidic mesophases. *Journal of molecular biology* **357**, 1605–1618 (2006).

83. Faizi, M., Zavřel, T., Loureiro, C., Červenỳ, J. & Steuer, R. A model of optimal protein allocation during phototrophic growth. *Biosystems* **166**, 26–36 (2018).

84. Zavřel, T., Sinetova, M. A., Búzová, D., Literáková, P. & Červenỳ, J. Characterization of a model cyanobacterium synechocystis sp. pcc 6803 autotrophic growth in a flat-panel photobioreactor. *Engineering in Life Sciences* **15**, 122–132 (2015).

85. Thiel, V., Tank, M. & Bryant, D. A. Diversity of Chlorophototrophic Bacteria Revealed in the Omics Era. *Annual Review of Plant Biology* **69**, annurev–arplant–042817–040500 (2018). URL http://www.annualreviews.org/doi/10.1146/annurev-arplant-042817-040500.

86. Hohmann-Marriott, M. F. & Blankenship, R. E. Evolution of photosynthesis. *Annual review of plant biology* **62**, 515–548 (2011).

87. Zubkov, M. V. Photoheterotrophy in marine prokaryotes. *Journal of Plankton Research* **31**, 933–938 (2009).

88. Panzer, S., Brych, A., Batschauer, A. & Terpitz, U. Opsin 1 and opsin 2 of the corn smut fungus ustilago maydis are green light-driven proton pumps. *Frontiers in microbiology* **10**, 735 (2019).

89. Marchetti, A., Catlett, D., Hopkinson, B. M., Ellis, K. & Cassar, N. Marine diatom proteorhodopsins and their potential role in coping with low iron availability. *ISME Journal* **9**, 2745–2748 (2015). URL http://dx.doi.org/10.1038/ismej.2015.74.

90. Gómez-Consarnau, L. *et al.* Proteorhodopsin Phototrophy Promotes Survival of Marine Bacteria during Starvation. *PLOS Biology* **8**, 1–10 (2010). URL https://doi.org/10.1371/journal.pbio.1000358.

91. Gómez-Consarnau, L. *et al.* Proteorhodopsin Phototrophy Promotes Survival of Marine Bacteria during Starvation. *PLOS Biology* **8**, 1–10 (2010). URL https://doi.org/10.1371/journal.pbio.1000358.

92. Basan, M. *et al.* Overflow metabolism in escherichia coli results from efficient proteome allocation. *Nature* **528**, 99–104 (2015).

93. Flamholz, A., Noor, E., Bar-Even, A., Liebermeister, W. & Milo, R. Glycolytic strategy as a tradeoff between energy yield and protein cost. *Proceedings of the National Academy of Sciences of the United States of America* **110**, 10039–10044 (2013).

94. Hui, S. *et al.* Quantitative proteomic analysis reveals a simple strategy of global resource allocation in bacteria. *Molecular systems biology* **11** (2015).

95. Scott, M., Klumpp, S., Mateescu, E. M. & Hwa, T. Emergence of robust growth laws from optimal regulation of ribosome synthesis. *Molecular systems biology* **10** (2014).

96. Erickson, D. W. *et al.* A global resource allocation strategy governs growth transition kinetics of escherichia coli. *Nature* **551**, 119–123 (2017).

97. Wortel, M. T., Noor, E., Ferris, M., Bruggeman, F. J. & Liebermeister, W. Metabolic enzyme cost explains variable trade-offs between microbial growth rate and yield. *PLoS computational biology* **14**, e1006010 (2018).

98. Zavřel, T. *et al.* Quantitative insights into the cyanobacterial cell economy. *Elife* **8**, e42508 (2019).

99. Faizi, M. & Steuer, R. Optimal proteome allocation strategies for phototrophic growth in a light-limited chemostat. *Microbial cell factories* **18**, 165 (2019).

100. Connell, J. H. & Slatyer, R. O. Mechanisms of succession in natural communities and their role in community stability and organization. *The American Naturalist* **111**, 1119–1144 (1977).

101. Fukami, T. Historical contingency in community assembly: integrating niches, species pools, and priority effects. *Annual Review of Ecology, Evolution, and Systematics* **46**, 1–23 (2015).

102. De Meester, L., Vanoverbeke, J., Kilsdonk, L. J. & Urban, M. C. Evolving perspectives on monopolization and priority effects. *Trends in Ecology & Evolution* **31**, 136–146 (2016).

103. Cavender-Bares, J., Ackerly, D. D., Hobbie, S. E. & Townsend, P. A. Evolutionary legacy effects on ecosystems: Biogeographic origins, plant traits, and implications for management in the era of global change. *Annual Review of Ecology, Evolution, and Systematics* **47**, 433–462 (2016).

104. Mori, M., Marinari, E. & De Martino, A. A yield-cost tradeoff governs escherichia coli's decision between fermentation and respiration in carbon-limited growth. *NPJ systems biology and applications* **5**, 1–9 (2019).

105. Li, Y., Petrov, D. A. & Sherlock, G. Single nucleotide mapping of trait space reveals pareto fronts that constrain adaptation. *Nature ecology & evolution* 1–13 (2019).

106. Sancar, A. Structure and function of photolyase and in vivo enzymology: 50th anniversary. *Journal of Biological Chemistry* **283**, 32153–32157 (2008).

107. Sorigué, D. *et al.* An algal photoenzyme converts fatty acids to hydrocarbons. *Science* **357**, 903–907 (2017).

108. Kritsky, M. S., Telegina, T. A., Vechtomova, Y. L. & Buglak, A. A. Why flavins are not competitors of chlorophyll in the evolution of biological converters of solar energy. *International journal of molecular sciences* **14**, 575–593 (2013).

109. Rothschild, L. J. The evolution of photosynthesis... again? *Philosophical Transactions of the Royal Society B: Biological Sciences* **363**, 2787–2801 (2008).

110. Shalaeva, D. N., Galperin, M. Y. & Mulkidjanian, A. Y. Eukaryotic g protein-coupled receptors as descendants of prokaryotic sodium-translocating rhodopsins. *Biology direct* **10**, 63 (2015).

111. Sánchez-Baracaldo, P. & Cardona, T. On the origin of oxygenic photosynthesis and cyanobacteria. *New Phytologist* **225**, 1440–1446 (2020).

112. Cardona, T. & Rutherford, A. W. Evolution of photochemical reaction centres: more twists? *Trends in plant science* (2019).

113. GRANICK, S. Evolution of heme and chlorophyll. In Bryson, V. & Vogel, H. J. (eds.) *Evolving Genes and Proteins*, 67 – 88 (Academic Press, 1965). URL http://www.sciencedirect.com/science/article/pii/B9781483227344500140.

114. Chew, A. G. M. & Bryant, D. A. Chlorophyll biosynthesis in bacteria: The origins of structural and functional diversity. *Annual Review of Microbiology* **61**, 113–129 (2007). URL https://doi.org/10.1146/annurev.micro.61.080706.093242. PMID: 17506685.

115. Xiong, J. & Bauer, C. E. A cytochrome b origin of photosynthetic reaction centers: an evolutionary link between respiration and photosynthesis. *Journal of molecular biology* **322**, 1025–1037 (2002).

116. Epel, B. & Butler, W. L. Cytochrome a3: Destruction by light. *Science* **166**, 621–622 (1969).

117. Robertson, J. B., Davis, C. R. & Johnson, C. H. Visible light alters yeast metabolic rhythms by inhibiting respiration. *Proceedings of the National Academy of Sciences* **110**, 21130–21135 (2013).

118. Carlile, M. Prokaryotes and eukaryotes: strategies and successes. *Trends in Biochemical Sciences* **7**, 128–130 (1982).

119. Zaremba-Niedzwiedzka, K. *et al.* Asgard archaea illuminate the origin of eukaryotic cellular complexity. *Nature* **541**, 353–358 (2017).

120. Stairs, C. W. & Ettema, T. J. The archaeal roots of the eukaryotic dynamic actin cytoskeleton. *Current Biology* **30**, R521–R526 (2020).

121. Penev, P. I. *et al.* Supersized ribosomal rna expansion segments in asgard archaea. *Genome biology and evolution* **12**, 1694–1710 (2020).

122. Neveu, E., Khalifeh, D., Salamin, N. & Fasshauer, D. Prototypic snare proteins are encoded in the genomes of heimdallarchaeota, potentially bridging the gap between the prokaryotes and eukaryotes. *Current Biology* (2020).

123. Shiratori, T., Suzuki, S., Kakizawa, Y. & Ishida, K.-i. Phagocytosis-like cell engulfment by a planctomycete bacterium. *Nature Communications* **10**, 5529 (2019). URL http://dx.doi.org/10.1038/s41467-019-13499-2http://www.nature.com/articles/s41467-019-13499-2.

 doi:10.20944/preprints202011.0700.v4

124. Sagulenko, E. *et al.* Structural studies of planctomycete gemmata obscuriglobus support cell compartmentalisation in a bacterium. *PLoS One* **9** (2014).

125. Boedeker, C. *et al.* Determining the bacterial cell biology of planctomycetes. *Nature communications* **8**, 1–14 (2017).

126. Mahajan, M. *et al.* Paralogization and new protein architectures in planctomycetes bacteria with complex cell structures. *Molecular biology and evolution* **37**, 1020–1040 (2020).

127. Strous, M. *et al.* Missing lithotroph identified as new planctomycete. *Nature* **400**, 446–449 (1999).